



### **Science Arts & Métiers (SAM)**

is an open access repository that collects the work of Arts et Métiers Institute of Technology researchers and makes it freely available over the web where possible.

This is an author-deposited version published in: <https://sam.ensam.eu>  
Handle ID: <http://hdl.handle.net/10985/14439>

#### **To cite this version :**

Baris AYKENT, Andras KEMENY, Frédéric MERIENNE, Jean-Rémy CHARDONNET - Angular Velocity Perception Threshold and Sense of Presence for a Three Degrees of Freedom (DOF). Driving Simulator in Virtual Environment - SAE Technical Paper n°2018-01-5043, p.1-11 - 2018

# Angular Velocity Perception Threshold and Sense of Presence for a Three Degrees of Freedom (DOF) Driving Simulator in Virtual Environment

**Baris Aykent** Hexagon Studio

**Jean-Remy Chardonnet and Frederic Merienne** Arts et Metiers ParisTech

**Andras Kemeny** Arts et Metiers ParisTech and Renault SAS

**Citation:** Aykent, B., Chardonnet, J.-R., Merienne, F., and Kemeny, A., "Angular Velocity Perception Threshold and Sense of Presence for a Three Degrees of Freedom (DOF) Driving Simulator in Virtual Environment," SAE Technical Paper 2018-01-5043, 2018, doi:10.4271/2018-01-5043.

## Abstract

Angular velocity perception plays an important role for a better sense of presence in driving simulators. This paper deals with the angular velocity perception threshold and sense of presence.

A three degrees of freedom (DOF: roll, pitch, and heave) driving simulator, a motion tracking sensor, a driving simulation software, and self-prepared questionnaires were used.

Due to the subjective assessments, there were no significant differences between static and dynamic platform types. Eight different cases were investigated with respect to visual and inertial factors (field of view (FOV) and motion platform).

Subjective evaluations showed that there were no significant differences between static and dynamic conditions. Lower FOV, static platform, stereo vision condition has provided the best condition (best realism depending on objective-subjective measure relationship).

## Introduction

### Context

In driving simulation, sense of presence is a very well-known and important topic to study further on, and therefore it is required to develop systems and/or methods to increase it [1, 2].

### State of the Art

Improving the realism of motion cueing is realizable by using other sensory cues, for example, visual cues. Body orientation's perception might be affected by visual cues. Due to [3, 4], visual cues had more elevated level of influences on the perceived orientation than the sensed direction of gravity named as "vection" (visually induced illusion of angular or linear self-motion). A negative correlation has resulted in vertical movement between individual vestibular threshold and vection onset latency (VOL): the lower the vestibular threshold, the longer the delay in vection [3, 5, 6] (vection onset latency and vestibular thresholds (VOL)).

The impact of vestibular stimulation with various angular accelerations and velocities on perceiving the visual motion direction was examined. Fixed accelerations resulting in diverse angular velocities and fixed angular velocities obtained at diverse accelerations were merged in 20 healthy participants. It was shown that perception thresholds significantly raised with increasing angular velocity. It has also resulted that raised

acceleration had no significant influence on the perception thresholds. It was concluded that merely the achieved angular velocity was the dominant factor in the treatment of vestibular-visual interaction [7].

A study was accomplished to investigate the perceptual relationships between angular and linear perception thresholds during simultaneous rotation and translation on a curved path. Rotation thresholds augmented vaguely, however not significantly, with synchronous linear velocity magnitude. Yaw rotation perception threshold was determined as  $1.45 \pm 0.81$  °/s ( $3.49 \pm 1.95$  °/s<sup>2</sup>). Translation thresholds elevated significantly with raising magnitude of synchronous angular velocity. These findings suggest that aware perception might not separate estimates of linear and angular motion parameters during curved-path movement [8].

A turning cabin driving simulator was constructed and multiple projectors were used together with a 360-degree cylindrical screen to generate a display. Driver participants reported a significant less amount of simulator sickness when the simulator cabin turned around the yaw axis. The results emphasized that a much higher amount of optical flow was experienced by all drivers when the cabin was static [9].

A research was realized in order to compare different visual conditions [10]. A first experiment was composed of three DOF (roll, pitch, and heave) at computer automatic virtual environment (CAVE) as CAVE active stereo and mono visions as well as head-mounted display (HMD) vision. The stereo and mono visual cases' performances differed from each other very indistinctly. HMD experience resulted in

weaker speed perception and velocity was harder to maintain; furthermore HMD required more amount of lateral control effort to maneuver through the cones. Nevertheless, HMD yielded a higher accuracy for stopping at a predefined line. As a conclusion, subjects did not make a clear predilection for any of the visual conditions [10].

A second experiment included comparing the driving performance between the CAVE and six DOF ride motion simulator (RMS). Driving performances between the CAVE and RMS were highly similar. Driving session appeared to be more consistent between the first and second drives on the RMS comparing to the CAVE. During the curvature driving, it required more level of control by the participants to guard the trajectory. The speeds were underestimated for the both cases (CAVE and RMS). Simulator sickness measures were approximately similar between the RMS and CAVE cases. The relief-band had the role of lowering the simulator sickness symptoms between the first and second drives [10].

Simulators with motion platform systems were used to put the driver in the loop with an existence of a motion feedback from motion platforms for diverse kinds of DOFs. The type of the motion platform and its related motion envelope was a main element for the capability to satisfy specific motion cues. Algorithms for three types of motion systems with the eight DOF systems (six DOF, x and y rails), six DOF systems (roll, pitch, yaw, surge, sway, and heave), and three DOF systems (roll, pitch, and linear rail) were discussed [11].

A motion-cueing strategy used for a dynamic simulator with three DOF (roll, pitch, and yaw) to accomplish the roll, pitch, yaw, surge, and sway motions (five DOF) by using an online optimization algorithm was investigated in [12]. Furthermore, experiments were introduced to show the validity of the five DOF motion platform. By introducing the constrained optimization real-time optimal motion-cueing algorithm (ROMA), the motion control does not ensure merely a precise cue to the participant but also secures the mechanical construction of the motion platform. Tests were realized online and revealed that the proposed strategy brings much more realistic movements than the classical algorithm does for a three DOF motion platform. The proposed motion cueing is in general applicable to all motion simulators with rotational three DOF [13].

Eight low-cost non-vestibular motion-cueing systems were evaluated and compared with respect to the driver performance as the cueing system disengaged: seat belt tensioning system, vibrating steering wheel, motion seat, screeching tire sound, beeping sound, road noise, vibrating seat, and pressure seat. The results indicated that these systems were advantageous in reducing velocity and acceleration and they enhanced lane-keeping and/or stopping accuracy. The seat belt tensioning system had a particularly higher impact on driver braking performance. This system decreased driving velocity, raised stopping distance, lowered maximum deceleration, and enhanced stopping preciseness. It was deduced that low-cost non-vestibular motion cueing could be a preliminary option in order to ameliorate simulator's cabin characteristics so that it better complies with real-life driving situation [14].

"CAVE" is a multiple-face prism with images on each surface used in virtual reality (VR) environments. It has been rated as being adequate and ample as the "immersive" simulation of VR comparing to the insufficient head-mounted

displays (HMDs) in that domain [15, 16, 17, 18]. Nevertheless, current HMDs are able to rival with many CAVEs [19].

A study was accomplished in order to compare the levels of presence and anxiety, fear that was visualized by using a CAVE and a head-mounted display (HMD) [20]. The experiments for the two visualization systems were realized to compare their impacts on the participants (non-phobic users). After having experienced each visualization system (HMD or CAVE), the participants were requested to complete an adapted Slater et al. questionnaire [20, 21]. Due to [20], the CAVE yielded a more elevated level of presence for users. The results depicted that the CAVE increased anxiety more than the HMD did [20].

An experimental procedure was discussed in order to evaluate the HMD Oculus and three LCD screens (ECO<sub>2</sub> static driving simulator) for a specific driving scenario with respect to simulation sickness. HMD Oculus caused a more elevated level of nausea, dizziness, and eyestrain than those with ECO<sub>2</sub> static driving simulator. In terms of headache, mental pressure, fear, and uneasiness, no significant difference was obtained between HMD Oculus and ECO<sub>2</sub> static driving simulator, although the mean values of those in HMD Oculus were all higher than those in ECO<sub>2</sub> driving simulator. Regarding the visual quality, ECO<sub>2</sub> static driving simulator was assessed significantly better than HMD Oculus. With regard to the immersive impression, no significant difference was found between two devices [21].

## Scientific Issue

In driving simulation, there are mainly two stimuli as visual environment and motion platform of the simulator as whether it is active or passive. The reason why angular velocity has been investigated was:

- Since it is an important factor for motion perception, its relation with the sense of presence gives an idea about realism.

The questions to be investigated in this research were:

- "What is the value of angular velocity perception threshold in the driving simulation in terms of sensory stimuli?" (It refers to the angular velocity sensitivity for the feeling of immersion in driving simulators.)
- "How different the sense of presence is perceived in the driving simulation with respect to sensory stimuli?"
- "Is there any relationship between angular velocity perception threshold and the sense of presence in the driving simulation with regard to sensory stimuli?"

## Plan of the Article

There are two important topics to investigate, in terms of driving simulation, which are the angular velocity threshold and sense of presence for a three DOF (roll, pitch, heave) driving simulator that emphasizes this research paper. The paper is organized as follows: Section 2 describes "methods and materials," section 3 highlights "objective measures," section 4 explains "subjective measures," section 5 deals with "results and discussion," and finally section 6 concludes this paper.

# Methods and Materials

## Proposed Approach

The objective of the experiments in this paper is to investigate angular velocity thresholds (thetadot<sub>pt</sub>, pitch velocity perception threshold; phidot<sub>pt</sub>, roll velocity perception threshold; and psidot<sub>pt</sub>, yaw velocity perception threshold), their influence on sense of presence, and the comparison of sense of presence for the  $2^3 = 8$  different cases given in Table 1.

Therefore, a scenario has been established in the driving simulation software SCANeRstudio version 1.4 that enables building a specific driving incidence. The scenario is composed of traffic situation, buildings, several roundabouts, curvatures, and the environmental surroundings.

For this study, merely the sustained velocities (angular velocity, yaw velocity) were taken into account.

The term “sense of presence” refers to being or sensing more realistic in the virtual environment.

The three DOF motion system (roll, pitch, and heave), used in this paper, is composed of four electric actuators located at the four corners of the cockpit. This system has a faster response than the two DOF motion system (roll, pitch) including in the basic package (100 Hz possible vibrations). It also helps to make elevations on the vertical axis, which takes an important role to make relief feel realistically. This system is being exploited by actuators of D-BOX [22].

The performance of this three DOF motion platform is shown in Table 2.

The control of this motion platform is provided by the PC and it comes with the cockpit.

The construction is made up of aluminum profiles. It maintains a realistic cockpit altitude, identical to that of a real vehicle.

The CAVE system at Institut Image of Arts et Métiers ParisTech (modular virtual environment (MoVE); it is a device consisting of a visual immersion stereoscopic capture of the user's position) has the characteristics as given in Table 3.

The MoVE is composed of cubic shape surrounded walls with 3 m side, with four faces immersive, passive stereoscopic visualization on Infitec projectors: Projection Design F30SX+.

**TABLE 1** Design of experiments.

|  | Inertial stimulus |
|--|-------------------|
|  | Static/dynamic    |
| Mono/stereo visions  |                   |
| FOV 1 (horizontal, 60°; vertical, 60°)/FOV 2 (horizontal, 220°; vertical, 90°) |                   |

**TABLE 2** The characteristics of this three DOF motion platform.

|                                |  |
|--------------------------------|--|
| Maximum vertical acceleration  | Limited to 1 g (9.81 m/s <sup>2</sup> ) through the software |
| Stroke of each actuator        | 35 mm  |
| Maximum speed of each actuator | 100 mm/s   |
| Load capacity                  | 455 kg   |
| Roll (estimate)                | ±3.2°  |
| Pitch (estimate)               | ±2.5°  |

**TABLE 3** Characteristics of the MoVE.

|                                 |   |
|---------------------------------|---|
| Tracking system                 | Four infrared cameras tracking ArtTrack2  |
| Rendering system with computers | Two rendering servers: a calculator with 2x Nvidia Quadro Plex D7000 and a computer with 3x AMD FirePro V9800   |
| Audio system                    | The spatial audio with a 2.1 kit  |
| Projector system                | It has a structure that consists of eight video projectors from “projectiondesign” which was acquired by “Barco.” It has a resolution maximum up to 1920px1200p. Its native resolution is 1400px1050p with an aspect ratio of 4:3 |

Figure 1 illustrates the three DOF (with roll, pitch, and heave motion) dynamic driving simulator in a four-face CAVE system. Figure 2 shows the used classical motion-cueing algorithm from a hexapod (six DOF) motion platform [21, 23], and it was adapted to a three DOF motion platform. For the real-time head tracking feature, advanced real-time tracking (ART) device was utilized.

For each case, the angular velocity perception thresholds (roll velocity  $\omega_x$ , pitch velocity  $\omega_y$ , yaw velocity  $\omega_z$  in °/s as objective metrics) that depend on the vehicle as well as the vestibular dynamics and the sense of presence (subjective measures through questionnaires) of the drivers are measured. Figure 3 shows the sensor XSens that is used to measure the head (vestibular related) dynamics data (attached to the headphone from right) [21, 24, 27].

The effect of “the number of faces (FOV 1, FOV 2) in CAVE system,” “vision type (mono, stereo),” and “motion platform condition (static, dynamic)” is explained statistically for the driving simulation and the sense of presence for the subjects who participated in the experiments.

The mono vs. stereo vision was controlled from the projector system given in Table 3. The projectors themselves were having passive stereoscopic visualization characteristics, as of factory adjustments. In order to switch from stereo to mono vision, the passive stereoscopic visualization was inactivated during the experiments. FOV 1 (one face is on) and FOV 2 (four faces are on) properties were given in Table 1. The native resolution of the projectors as being 1400p X 1050p was used in the experiments with aspect ratio of 4:3.

Mono or stereo vision, static or dynamic platform, and FOV 1 and FOV 2 were the factors (variables) of which their effects had been investigated.

## Subjects

Figure 4 also depicts statistics for driving experience of the participants in the driving experiments.

Twenty-seven subjects (25 males and 2 females) aged  $32.74 \pm 7.82$  years old (mean  $\pm$  SD) and with driving experience of  $13.55 \pm 8.40$  years (mean  $\pm$  SD) participated in the experiments.

## Protocol

The subjects have driven the same scenario as given in Figure 4 on the dynamic simulator. The two-tailed Mann-Whitney U tests and the linear regression tests were achieved



**FIGURE 1** Three DOF (pitch, roll, heave) dynamic driving simulator during experiments: FOV 2 on left, FOV 1 on right.

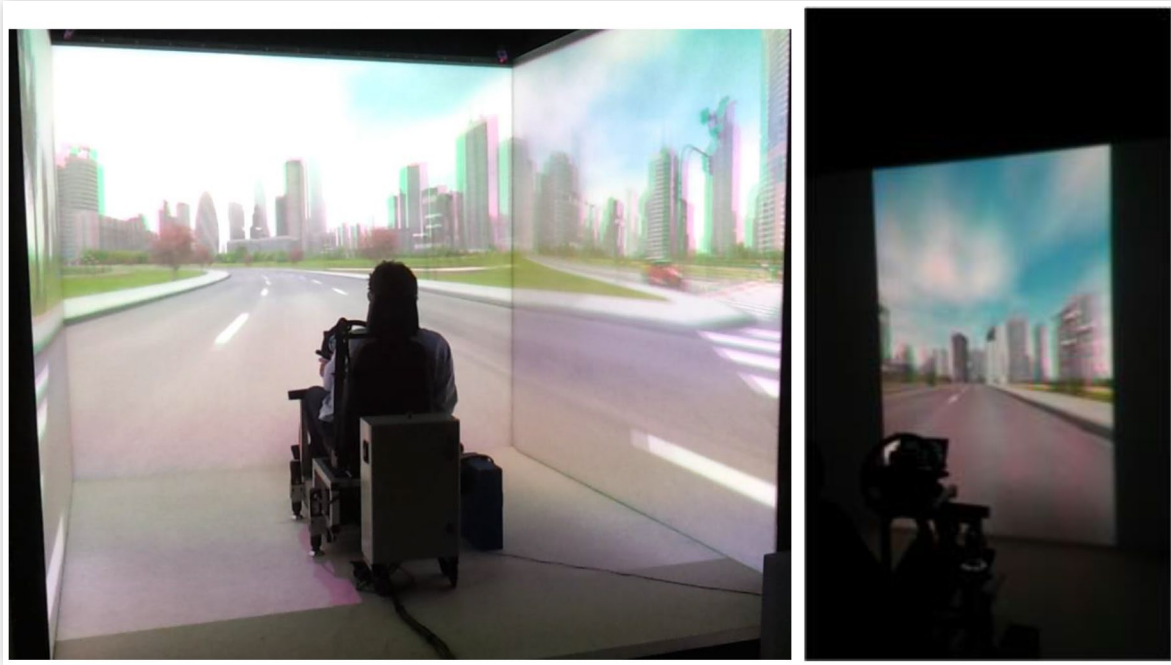
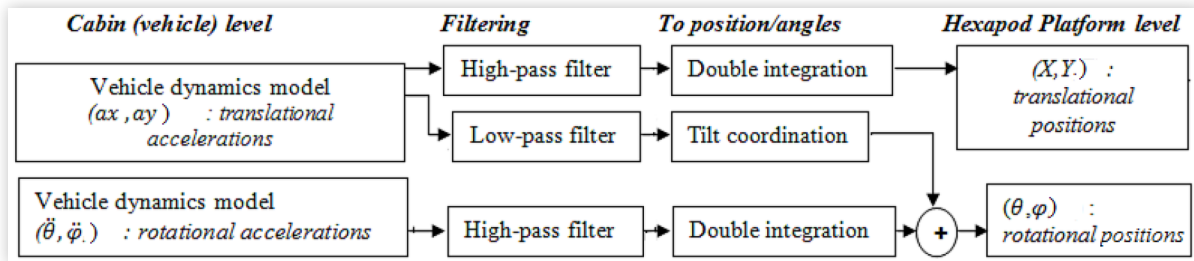


**FIGURE 2** Classical motion-cueing algorithm [1, 21].

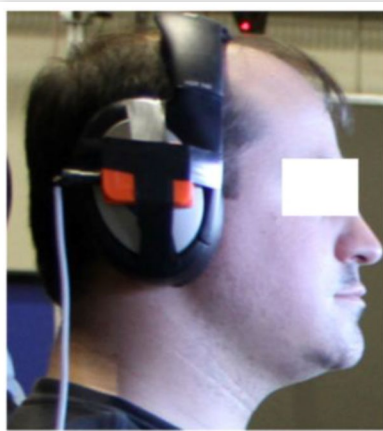


by using between subjects design. Each participant has driven the session for familiarization before the evaluation and measure sessions. The two-tailed Mann-Whitney U tests were used to evaluate the significance in difference for the subjective measures (via questionnaire), whereas the linear

regression tests were applied to obtain the correlation between vehicle and head level measures for getting yaw angular velocity perception threshold and also subjective measures and head level yaw angular velocity (see Figure 6).

The vehicle velocity (km/h) profile during the driving sessions and the vehicle trajectory (m × m) are shown in Figures 4a and 4b, respectively.

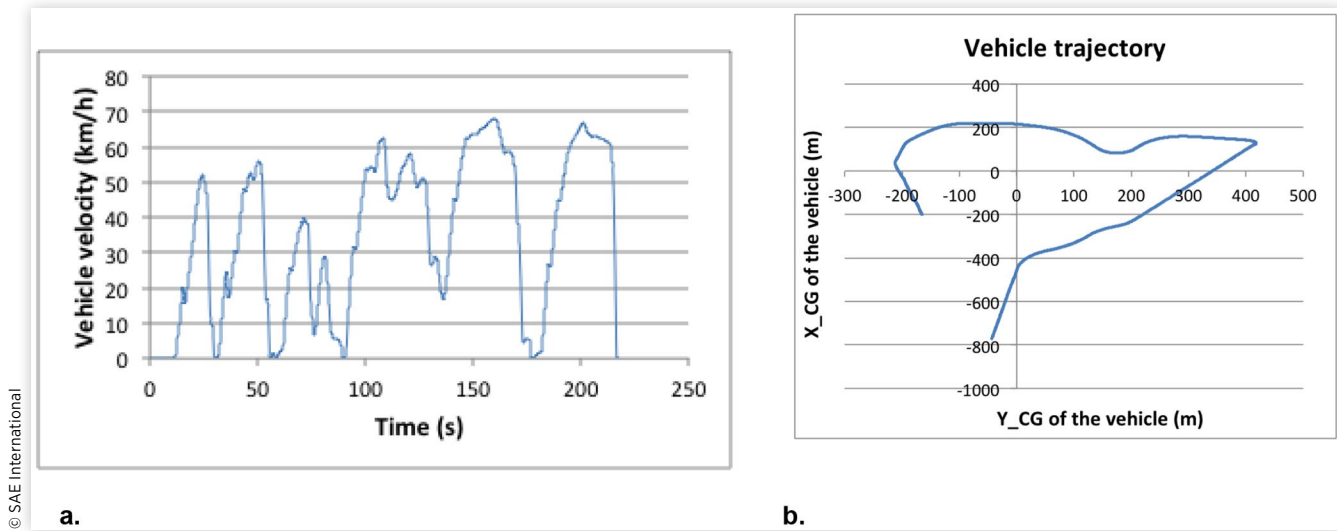
**FIGURE 3** Vestibular level data acquisition [1, 21, 24, 25].



## Objective Measures

The dynamics data of vehicle and head motions are all recorded in “.mat” files by using MATLAB. By constructing a Simulink model, the angular velocity data of vehicle and head (vestibular) were able to be processed. In order to evaluate the angular velocity thresholds as of pitch velocity, as of roll velocity, and as of yaw velocity thereafter to assess the self-reports for the sense of presence, curve fitting tool (centered and scaled first-degree polynomial bi-square robust with linear least squares fitting option was used) [26] and two-tailed Mann-Whitney U tests are, respectively, employed in MATLAB [27].

**FIGURE 4** (a) Vehicle velocity (km/h) profile during the driving sessions and (b) vehicle CG (center of gravity) trajectory during the driving experiments.



First-degree polynomial fitting between sets of data is for predicting how associated are those two data with each other, in other words that is used to indicate the linear relationship of two sets of angular velocities in order to determine the angular velocity thresholds [26].

In order to analyze the significance in differences of the subjective ratings for the sense of presence between the mono vision and stereo vision type data, another analysis method (bilateral Mann-Whitney U test) is used in MATLAB. Mann-Whitney U test can evaluate two sets of data without condition on sample size [27].

## Subjective Measures

The subjective measure is defined as conducting a questionnaire evaluation for all subjects at the end of each driving simulation phase. It was not a direct measure of the perception but instead it was the measure of reaction to the simulation. These issues are associated with the subject's self-reports on the sense

of presence. Questions focus on the rating of experienced visual information, acceleration information, steering wheel feeling, braking information, etc. Table 4 lists the questions after each driving phase. The purposed questionnaire in this report has been built and modified from the following sources [23].

The participant had to report on his/her own for each of these questions with a value. This value should reflect psycho-physical sense of presence during the experiment (from 1 to 10). Thereafter, these values were statistically analyzed.

## Results and Discussion

The results of this research discuss the driving simulation comparison between mono and stereo type visions, the comparison between dynamic and static platform conditions, and the comparison between FOV 1 and FOV 2 in the CAVE. The MATLAB/Simulink is used to calculate the data and present the results.

$\omega_x$ ,  $\omega_y$ , and  $\omega_z$  were measured from the participants' right ear levels (thetadot\_vest, phidot\_vest, psidot\_vest) for the same driven scenario for the static and dynamic platforms via using the sensor in Figure 3 [21] during the experiments.

Figure 5 summarizes the method and the data analysis used in the paper. Angular velocities (roll velocity, pitch velocity, and yaw velocity) from the vehicle level and the head (vestibular) level were collected during the experiments. Then from MATLAB ("cftool": curve fitting toolbox) curve fitting was realized between head and vehicle angular velocity data as with centered and scaled first-degree polynomial bi-square robust with linear least squares fitting option (Table 5, Figure 6). The mean value of the fit (the magnitude as absolute value) gives the angular velocity perception threshold. If there is significant relationship between "sense of presence self-report" and "angular velocity perception threshold," it indicates that this angular velocity perception threshold is realistic.

**TABLE 4** List of questions.

| Questions | Expression of question                     |  |
|-----------|--|--|
| Q1        | Visual information                         | (1, very bad; 10, very well)               |
| Q2        | Acceleration information                   | (1, very bad; 10, very well)               |
| Q3        | Steering wheel feeling                     | (1, very disagreeable; 10, very agreeable) |
| Q4        | Braking information                        | (1, very bad; 10, very well)               |
| Q5        | Roll motion                                | (1, too little; 10, too strong)            |
| Q6        | Pitch motion                               | (1, too little; 10, too strong)            |
| Q7        | Driving impression during straight forward | (1, very bad; 10, very well)               |
| Q8        | Driving impression during curvature        | (1, very bad; 10, very well)               |
| Q9        | Entire driving impression                  | (1, very bad; 10, very well)               |

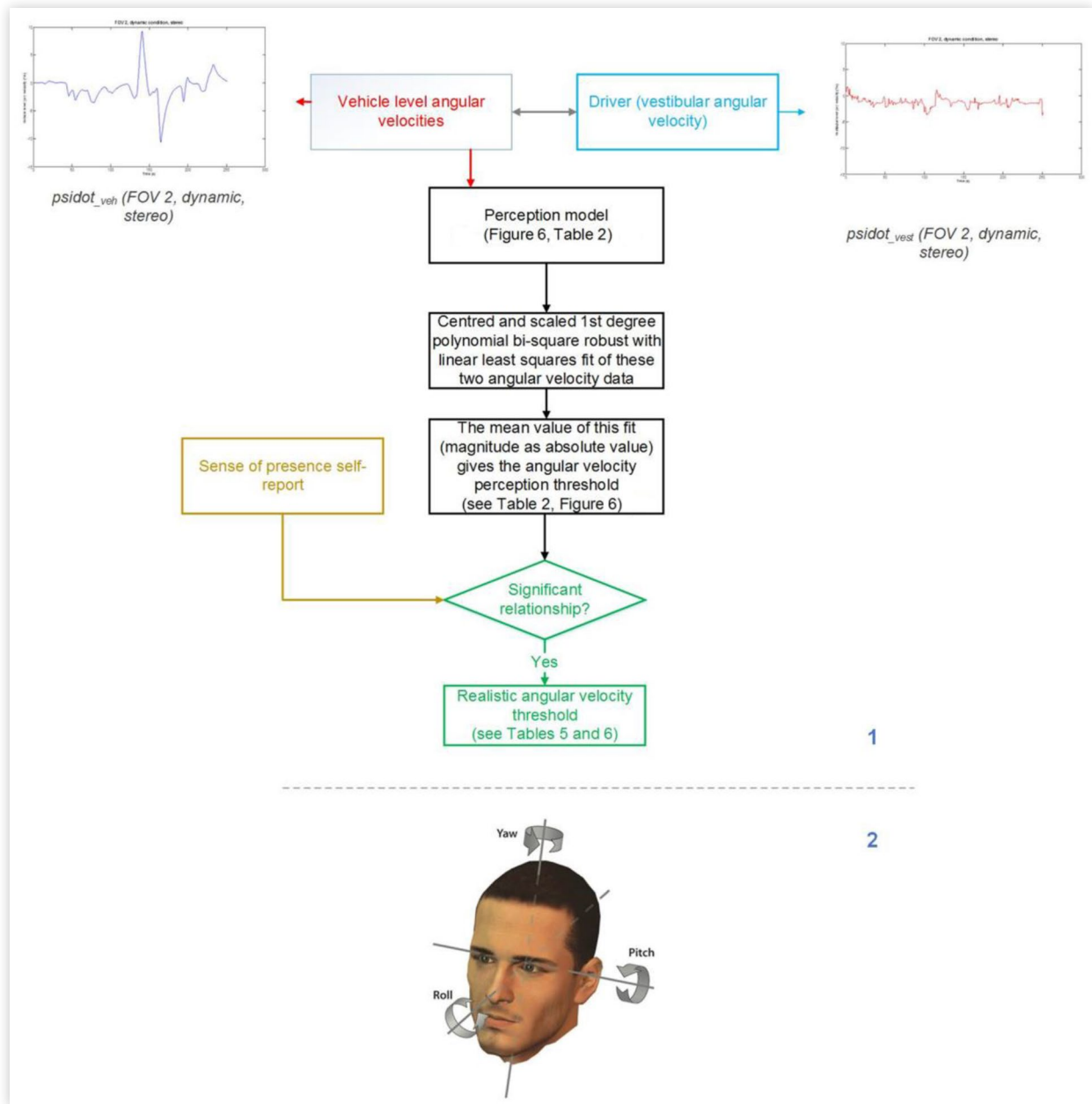
**FIGURE 5** Method and data analysis.

Table 5 shows the pitch, the roll, and the yaw velocity perception thresholds. The thresholds were taken into account as in absolute values. SSE, sum of squared errors; RMSE, root mean squared error; and R-square are the terms coming from the curve fitting. For more information, the sources [26, 27] can be referred.

Upper part of Figure 6 depicts the time domain measures of yaw velocity for vehicle (blue curve) and vestibular (red curve) levels. Below part of Figure 6 shows the method proposed to identify the angular (pitch, roll, and yaw) velocity perception thresholds. The head movements (vestibular cues) and the vehicle movements were taken into account. Furthermore visuo-vestibular interaction (visuo, vehicle, and vestibular, head angular velocities) was investigated in Figure 6.

In below part of Figure 6, "psidot-vest" is the vestibular level measured yaw velocity in °/s, whereas the "psidot-veh" is the vehicle level (visual cues) yaw velocity in °/s. Blue line named "fit" is the curve fitting as with centered and scaled first-degree polynomial bi-square robust with linear least squares fitting option. This fit shown with blue line in Figure 6 specifies the (yaw) angular velocity perception threshold. In Figure 6, the ordinate values of the blue line correspond to the angular velocities matching to the vehicle yaw velocities.

## Subjective Analysis

**Comparison of Mono Type Vision with Stereo Type Vision** The subjective evaluation results have been

**TABLE 5** Perception threshold for angular velocities.

|       |                               | Static condition head/vehicle |                  |                  |                  |                  |                  | Dynamic condition head/vehicle |                  |                  |                  |                  |                  |
|-------|-------------------------------|-------------------------------|------------------|------------------|------------------|------------------|------------------|--------------------------------|------------------|------------------|------------------|------------------|------------------|
|       |                               | Mono vision                   |                  |                  | Stereo vision    |                  |                  | Mono vision                    |                  |                  | Stereo vision    |                  |                  |
|       |                               | $\omega_{x\_pt}$              | $\omega_{y\_pt}$ | $\omega_{z\_pt}$ | $\omega_{x\_pt}$ | $\omega_{y\_pt}$ | $\omega_{z\_pt}$ | $\omega_{x\_pt}$               | $\omega_{y\_pt}$ | $\omega_{z\_pt}$ | $\omega_{x\_pt}$ | $\omega_{y\_pt}$ | $\omega_{z\_pt}$ |
| FOV 1 | Lower 95% confidence interval | 0.3°/s                        | 1.19°/s          | 1.26°/s          | 0.5°/s           | 0.91°/s          | 1.51°/s          | 0.77 °/s                       | 1.14 °/s         | 1.25 °/s         | 0.69°/s          | 0.68°/s          | 1.55°/s          |
|       | Mean                          | 0.31°/s                       | 1.21°/s          | 1.3°/s           | 0.51°/s          | 0.93°/s          | 1.54°/s          | 0.78 °/s                       | 1.15 °/s         | 1.27 °/s         | 0.69°/s          | 0.7°/s           | 1.57°/s          |
|       | Upper 95% confidence interval | 0.33°/s                       | 1.24°/s          | 1.34°/s          | 0.52°/s          | 0.95°/s          | 1.57°/s          | 0.8 °/s                        | 1.17 °/s         | 1.29 °/s         | 0.7°/s           | 0.72°/s          | 1.59°/s          |
|       | SSE                           | 39                            | 85.88            | 205.5            | 14.8             | 60.56            | 123.9            | 17.79                          | 42.82            | 67.59            | 13.84            | 88.61            | 79.14            |
|       | R-square                      | 0.1557                        | 0.8894           | 0.546            | 0.5619           | 0.8569           | 0.6369           | 0.5516                         | 0.913            | 0.8233           | 0.8147           | 0.8192           | 0.8107           |
|       | RMSE                          | 0.2316                        | 0.3437           | 0.5317           | 0.1355           | 0.2741           | 0.3921           | 0.1571                         | 0.2437           | 0.3062           | 0.1304           | 0.3299           | 0.3118           |
|       |                               | Static condition head/vehicle |                  |                  |                  |                  |                  | Dynamic condition head/vehicle |                  |                  |                  |                  |                  |
|       |                               | Mono vision                   |                  |                  | Stereo vision    |                  |                  | Mono vision                    |                  |                  | Stereo vision    |                  |                  |
|       |                               | $\omega_{x\_pt}$              | $\omega_{y\_pt}$ | $\omega_{z\_pt}$ | $\omega_{x\_pt}$ | $\omega_{y\_pt}$ | $\omega_{z\_pt}$ | $\omega_{x\_pt}$               | $\omega_{y\_pt}$ | $\omega_{z\_pt}$ | $\omega_{x\_pt}$ | $\omega_{y\_pt}$ | $\omega_{z\_pt}$ |
| FOV 2 | Lower 95% confidence interval | 0.68°/s                       | 0.68°/s          | 1.3°/s           | 0.28°/s          | 0.52°/s          | 1.44°/s          | 0.74 °/s                       | 1.17 °/s         | 1.1 °/s          | 0.85 °/s         | 1.1 °/s          | 1.1 °/s          |
|       | Mean                          | 0.7°/s                        | 0.72°/s          | 1.36°/s          | 0.32°/s          | 0.56°/s          | 1.52°/s          | 0.76 °/s                       | 1.19 °/s         | 1.15 °/s         | 0.86 °/s         | 1.12 °/s         | 1.14 °/s         |
|       | Upper 95% confidence interval | 0.72°/s                       | 0.75°/s          | 1.4°/s           | 0.35°/s          | 0.59°/s          | 1.61°/s          | 0.78 °/s                       | 1.22 °/s         | 1.2 °/s          | 0.88 °/s         | 1.14 °/s         | 1.19 °/s         |
|       | SSE                           | 54.81                         | 154              | 340.7            | 112.9            | 102.5            | 668.7            | 95.65                          | 93.19            | 425.1            | 42.64            | 60.03            | 366.6            |
|       | R-square                      | 0.5712                        | 0.65             | 0.5816           | 0.5085           | 0.7934           | 0.5352           | 0.4062                         | 0.8537           | 0.2554           | 0.6104           | 0.8682           | 0.3101           |
|       | RMSE                          | 0.2798                        | 0.469            | 0.6977           | 0.4357           | 0.415            | 1.06             | 0.3389                         | 0.3345           | 0.7144           | 0.2274           | 0.2697           | 0.6666           |

explained due to the self-report of the participants just after each experimental session. Table 6 indicates subjective assessments for “the sense of presence” questionnaire in the case of “FOV 2, dynamic platform.”

Table 6 indicates the statistical difference analysis regarding the inertial factors (static or dynamic platform conditions). It does not show many options for multiple comparisons. The nonparametric tests in Table 6 show dual comparison from the left column to the right column (2×4). From Table 6, there were no significant differences between static and dynamic platform conditions for visual information, acceleration information, steering wheel feeling, braking information, driving impression during straight forward, driving impression during curvature, and entire driving impression. Merely, in terms of roll and pitch motion, the dynamic condition was perceived stronger than the static platform condition for the lower FOV with stereo vision. Furthermore, there were no significant differences between static and dynamic platform conditions in terms of subjective assessments for lower FOV with mono vision and for higher FOV with mono and stereo visions.

**Objective-Subjective Measure Relationships** Linear regression model was benefited to clarify the relationships between self-reports of the “sense of presence” (subjective measure) and the angular velocity thresholds (objective measure). The linear acceleration perception threshold was the “x1” and the self-report was the “y” for the linear regression model. MATLAB function “fitlm” [27] was used for the linear regression fitting (least squares method was chosen for the fitting).

Linear regression model:  $y \sim \text{Intercept} + x1$  [27]

The linear regression model is used to explain the objective (angular velocity perception thresholds) and subjective (self-reports for sense of presence) relationships.

Table 7 gives the results for objective (angular velocity perception thresholds) and subjective (self-reports for sense of presence) relationships. According to Table 7, “yaw velocity perception threshold” is significantly related to “entire driving impression” except for higher FOV with static platform and mono vision.

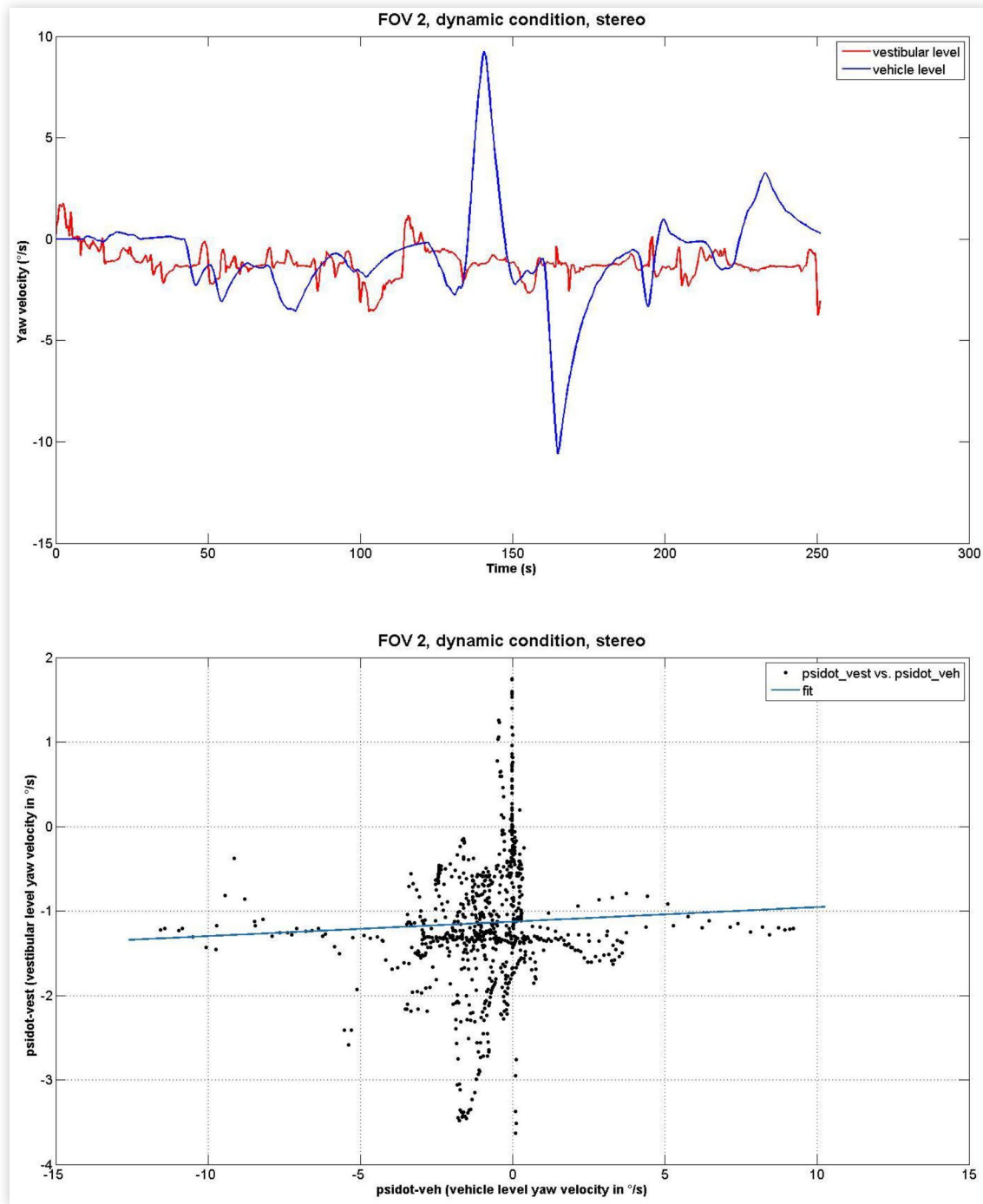
Table 8 gives the subjective weighted angular velocity perception threshold results. In Table 8, “d” refers to dynamic while “s” refers to static. Also subj (subjective), w (weighted), thetadot\_pt (pitch velocity perception threshold), phidot\_pt (lateral acceleration), and psidot\_pt (yaw velocity perception threshold) are given in Tables 7 and 8.

## Conclusion

The pitch, roll, and yaw angular velocity thresholds were discussed and how they can be identified from visuo-vestibular level angular velocities. Also, the subjective assessments were realized by using “sense of presence” questionnaires for the conditions.

As a result, it is seen that lower FOV, static platform, stereo vision condition has provided the best condition. In other words, the angular velocity (pitch, roll, and yaw velocity)



**FIGURE 6** Specifying the yaw velocity perception threshold from  $t = 0$  s (condition: FOV 2, dynamic condition, stereo).

thresholds have been significantly related to the self-report of entire driving impression for lower FOV, stereo vision at static platform condition. According to the subjective evaluations, there were no significant difference ( $p > 0.05$ ) between the static and the dynamic platform conditions apart from the "roll" and the "pitch" motion perception for lower FOV and stereo vision. The roll and the pitch motions were perceived stronger at the dynamic platform rather than the static platform condition at lower FOV and stereo vision. Except for higher FOV, static platform, and mono vision case, there was

a significant relationship between yaw velocity perception threshold and "entire driving impression." Pitch velocity perception thresholds were significantly related with "entire driving impression" for lower FOV, static platform, stereo vision; for lower FOV, dynamic platform, stereo vision; and for higher FOV, dynamic platform, stereo vision. Roll velocity perception thresholds were significantly related with "entire driving impression" for lower FOV, static platform, stereo vision; for higher FOV, static platform, mono vision; and for higher FOV, dynamic platform, mono vision.

**TABLE 6** Self-report for the sense of presence with respect to the platform condition.

|  | FOV 1<br>s_mono                  | FOV 1<br>d_mono | FOV 1<br>s_stereo                        | FOV 1<br>d_stereo | FOV 2<br>s_mono                  | FOV 2<br>d_mono | FOV 2<br>s_stereo                    | FOV 2<br>d_stereo |
|--|----------------------------------|-----------------|--|-------------------|----------------------------------|-----------------|--------------------------------------|-------------------|
| Visual information                         | 5.33<br>$U(27) : p = 1 > 0.05$   | 5.00            | 5.38<br>$U(27) : p = 0.9302 > 0.05$      | 5.33              | 6.33<br>$U(27) : p = 1 > 0.05$   | 6.33            | 7.06<br>$U(27) : p = 0.4467 > 0.05$  | 7.43              |
| Acceleration information                   | 5.33<br>$U(27) : p = 1 > 0.05$   | 5.00            | 5.69<br>$U(27) : p = 0.2520 > 0.05$      | 6.39              | 5.00<br>$U(27) : p = 0.5 > 0.05$ | 6.67            | 6.29<br>$U(27) : p = 0.07088 > 0.05$ | 6.43              |
| Steering wheel feeling                     | 6.00<br>$U(27) : p = 1 > 0.05$   | 5.33            | 6.19<br>$U(27) : p = 0.4130 > 0.05$      | 6.83              | 6.33<br>$U(27) : p = 0.8 > 0.05$ | 5.67            | 6.71<br>$U(27) : p = 0.6754 > 0.05$  | 7.00              |
| Braking information                        | 4.67<br>$U(27) : p = 0.6 > 0.05$ | 5.33            | 4.69<br>$U(27) : p = 0.2149 > 0.05$      | 5.61              | 4.67<br>$U(27) : p = 1 > 0.05$   | 5.67            | 4.94<br>$U(27) : p = 0.6456 > 0.05$  | 5.29              |
| Roll motion                                | 4.33<br>$U(27) : p = 0.6 > 0.05$ | 5.33            | 4.38<br>$U(27) : \mathbf{0.0337 < 0.05}$ | 5.89              | 4.33<br>$U(27) : p = 0.5 > 0.05$ | 6.33            | 5.29<br>$U(27) : p = 0.4649 > 0.05$  | 5.81              |
| Pitch motion                               | 4.00<br>$U(27) : p = 0.6 > 0.05$ | 5.33            | 3.81<br>$U(27) : \mathbf{0.0012 < 0.05}$ | 5.94              | 4.33<br>$U(27) : p = 0.7 > 0.05$ | 6.00            | 5.00<br>$U(27) : p = 0.2566 > 0.05$  | 5.86              |
| Driving impression during straight forward | 6.00<br>$U(27) : p = 1 > 0.05$   | 5.67            | 6.25<br>$U(27) : p = 0.1449 > 0.05$      | 7.22              | 6.00<br>$U(27) : p = 0.3 > 0.05$ | 7.00            | 7.00<br>$U(27) : p = 0.1314 > 0.05$  | 7.90              |
| Driving impression during curvature        | 4.67<br>$U(27) : p = 0.5 > 0.05$ | 6.00            | 5.25<br>$U(27) : p = 0.1950 > 0.05$      | 6.22              | 5.00<br>$U(27) : p = 0.8 > 0.05$ | 7.00            | 6.06<br>$U(27) : p = 0.1286 > 0.05$  | 6.95              |
| Entire driving impression                  | 5.00<br>$U(27) : p = 1 > 0.05$   | 5.67            | 5.81<br>$U(27) : p = 0.4970 > 0.05$      | 6.39              | 4.67<br>$U(27) : p = 0.3 > 0.05$ | 6.67            | 6.41<br>$U(27) : p = 0.2453 > 0.05$  | 7.05              |

**TABLE 7** Objective and subjective measure relationships.

| Entire driving impression | FOV 1<br>s_mono                     | FOV 1<br>d_mono                    | FOV 1<br>s_stereo            | FOV 1<br>d_stereo                  | FOV 2<br>s_mono                     | FOV 2<br>d_mono              | FOV 2<br>s_stereo                 | FOV 2<br>d_stereo                 |
|---------------------------|-------------------------------------|------------------------------------|------------------------------|------------------------------------|-------------------------------------|------------------------------|-----------------------------------|-----------------------------------|
| <i>thetadot_pt</i>        | p-value = 0.0732<br>> 0.05          | p-value = 0.121<br>> 0.05          | p-value = <b>0 &lt; 0.05</b> | p-value = <b>1.1e-07 &lt; 0.05</b> | p-value = 0.0524<br>> 0.05          | p-value = 0.0732<br>> 0.05   | p-value = 0.0524<br>> 0.05        | p-value = <b>0 &lt; 0.05</b>      |
| <i>phidot_pt</i>          | p-value = 0.121<br>> 0.05           | p-value = 1<br>> 0.05              | p-value = <b>0 &lt; 0.05</b> | p-value = 0.333<br>> 0.05          | p-value = <b>3.21e-08 &lt; 0.05</b> | p-value = <b>0 &lt; 0.05</b> | p-value = 0.0524<br>> 0.05        | p-value = 0.121<br>> 0.05         |
| <i>psidot_pt</i>          | p-value = <b>3.79e-08 &lt; 0.05</b> | p-value = <b>3.7e-08 &lt; 0.05</b> | p-value = <b>0 &lt; 0.05</b> | p-value = <b>0 &lt; 0.05</b>       | p-value = 0.0732<br>> 0.05          | p-value = <b>0 &lt; 0.05</b> | p-value = <b>0.0216 &lt; 0.05</b> | p-value = <b>0.0408 &lt; 0.05</b> |

**TABLE 8** Subjective weighted angular velocity perception threshold.

|                        | FOV 1<br>s_mono   | FOV 1<br>d_mono   | FOV 1<br>s_stereo   | FOV 1<br>d_stereo   | FOV 2<br>s_mono  | FOV 2<br>d_mono   | FOV 2<br>s_stereo   | FOV 2<br>d_stereo   |
|------------------------|---|---|---|---|--|---|---|---|
| Subj_w_<br>thetadot_pt | -   | -   | $0.93 \times (5.81 \div 10) = 0.54 \text{ }^\circ/\text{s}$ | $0.7 \times (6.39 \div 10) = 0.45 \text{ }^\circ/\text{s}$  | -  | -   | -   | $1.12 \times (7.05 \div 10) = 0.79 \text{ }^\circ/\text{s}$ |
| Subj_w_<br>phidot_pt   | -   | -   | $0.51 \times (5.81 \div 10) = 0.30 \text{ }^\circ/\text{s}$ | -   | $0.7 \times (4.67 \div 10) = 0.33 \text{ }^\circ/\text{s}$ | $0.76 \times (6.67 \div 10) = 0.51 \text{ }^\circ/\text{s}$ | -   | -   |
| Subj_w_<br>psidot_pt   | $1.3 \times (5 \div 10) = 0.65 \text{ }^\circ/\text{s}$ | $1.27 \times (5.67 \div 10) = 0.72 \text{ }^\circ/\text{s}$ | $1.54 \times (5.81 \div 10) = 0.89 \text{ }^\circ/\text{s}$ | $1.57 \times (6.39 \div 10) = 1.00 \text{ }^\circ/\text{s}$ | -  | $1.15 \times (6.67 \div 10) = 0.77 \text{ }^\circ/\text{s}$ | $1.52 \times (6.41 \div 10) = 0.97 \text{ }^\circ/\text{s}$ | $1.14 \times (7.05 \div 10) = 0.80 \text{ }^\circ/\text{s}$ |

## Contact Information

**Baris Aykent**  
Hexagon Studio  
Turkey  
[b.aykent@gmail.com](mailto:b.aykent@gmail.com)

## Definitions/Abbreviations

**FOV** - Field of view  
**DOF** - Degrees of freedom  
**HMD** - Head-mounted display  
**RMS** - Ride motion simulator  
**VOL** - Vection onset latency  
**ROMA** - Real-time optimal motion-cueing algorithm  
**VR** - Virtual reality  
**ECO<sub>2</sub>** - Ecological driving  
**MoVE** - Modular virtual environment  
**ART** - Advanced real-time training  
**SD** - Standard deviation  
**CG** - Center of gravity  
**Q<sub>n</sub>** - Questions; n = 1, ..., 9  
 **$\omega_x$**  - Roll velocity  
 **$\omega_y$**  - Pitch velocity  
 **$\omega_z$**  - Yaw velocity  
**thetadot\_vest** - Pitch velocity measured from the participants' right ear levels  
**phidot\_vest** - Roll velocity measured from the participants' right ear levels  
**psidot\_vest** - Yaw velocity measured from the participants' right ear levels  
**cftool** - Curve fitting toolbox of MATLAB  
**SSE** - Sum of squared errors  
**RMSE** - Root mean squared error  
**FOV1 s\_mono** - Field of view of horizontal 60°, vertical 60°, static platform, mono vision  
**FOV1 d\_mono** - Field of view of horizontal 60°, vertical 60°, dynamic platform, mono vision  
**FOV1 s\_stereo** - Field of view of horizontal 60°, vertical 60°, static platform, stereo vision  
**FOV1 d\_stereo** - Field of view of horizontal 60°, vertical 60°, dynamic platform, stereo vision  
**FOV2 s\_mono** - Field of view of horizontal 220°, vertical 90°, static platform, mono vision  
**FOV2 d\_mono** - Field of view of horizontal 220°, vertical 90°, dynamic platform, mono vision  
**FOV2 s\_stereo** - Field of view of horizontal 220°, vertical 90°, static platform, stereo vision  
**FOV2 d\_stereo** - Field of view of horizontal 220°, vertical 90°, dynamic platform, stereo vision

**thetadot\_pt** - Pitch velocity perception threshold

**phidot\_pt** - Roll velocity perception threshold

**psidot\_pt** - Yaw velocity perception threshold

## Acknowledgment

This research work was completed in the framework of the SI<sup>2</sup>M (Simulation Interface Homme Machine & Interaction) project.

## References

1. Aykent, B., Merienne, F., Guillet, C., Paillot, D. et al., "Motion Sickness Evaluation and Comparison for a Static Driving Simulator and a Dynamic Driving Simulator," *Proceedings of the Institution of Mechanical Engineers, Part D: Journal of Automobile Engineering* 228:818-839, 2014.
2. Aykent, B., Merienne, F., Paillot, D., and Kemeny, A., "The Role of Motion Platform on Postural Instability and Head Vibration Exposure at Driving Simulators," *Human Movement Science* 33:354-368, 2014.
3. Berger, D.R., Schulte-Pelkum, J., and Bühlhoff, H.H., "Simulating Believable forward Accelerations on a Stewart Motion Platform," *ACM Transactions on Applied Perception (TAP)* 7(1):5, 2010.
4. Akbari, B., "Motion Cueing Algorithms to Find Linear Self-Motion Thresholds on 6DOF Platforms," 2014.
5. Lepecq, J.C., Giannopulu, I., Mertz, S., and Baudonniere, P.M., "Vestibular Sensitivity and Vection Chronometry along the Spinal Axis in Erect Man," *Perception* 28(1):63-72, 1999.
6. Akbari, B., "Linear Self-Motion Thresholds on 6DOF Platforms," 2014.
7. Loose, R. and Probst, T., "Velocity not Acceleration of Self-Motion Mediates Vestibular-Visual Interaction," *Perception* 30(4):511-518, 2001.
8. MacNeilage, P.R., Turner, A.H., and Angelaki, D.E., "Canal-Otolith Interactions and Detection Thresholds of Linear and Angular Components during Curved-Path Self-Motion," *Journal of Neurophysiology* 104(2):765-773, 2010.
9. Mourant, R.R. and Yin, Z., "A Turning Cabin Simulator to Reduce Simulator Sickness," *IS&T/SPIE Electronic Imaging* (International Society for Optics and Photonics, Feb. 2010), 752503.
10. Mollenhauer, M.A., Romano, R.A., and Brumm, B., "The Evaluation of a Motion Base-Driving Simulator in a CAVE at TACOM," Realtime Technologies Inc., Fort Collins CO, 2004.
11. Fischer, M., Sehammar, H., and Palmkvist, G., "Applied Motion Cueing Strategies for Three Different Types of Motion Systems," *Journal of Computing and Information Science in Engineering* 11(4):041008, 2011.
12. Manek, D., "Effects of Visual Displays on 3d Interaction in Virtual Environments," Doctoral dissertation, Virginia Polytechnic Institute and State University, 2004.

13. Chang, Y.H., Liao, C.S., and Chieng, W.H., "Optimal Motion Cueing for 5-DOF Motion Simulations via a 3-DOF Motion Simulator," *Control Engineering Practice* 17(1):170-184, 2009.
14. De Groot, S., de Winter, J.C., Mulder, M., and Wieringa, P.A., "Nonvestibular Motion Cueing in a Fixed-Base Driving Simulator: Effects on Driver Braking and Cornering Performance," *Presence: Teleoperators and Virtual Environments* 20(2):117-142, 2011.
15. Shapiro, M., "Comparing User Experience in a Panoramic HMD vs. Projection Wall Virtual Reality System," Tech. Rep., Sensics, Inc., 2006.
16. Tossavainen, T., "Comparison of CAVE and HMD for Visual Stimulation in Postural Control Research," *Studies in Health Technology and Informatics* 98:385-387, 2004.
17. Kim, K., Rosenthal, M.Z., Zielinski, D., and Brady, R., "Comparison of Desktop, Head Mounted Display, and Six Wall Fully Immersive Systems Using a Stressful Task," *Virtual Reality Short Papers and Posters (VRW)*, 2012 IEEE, IEEE, Mar. 2012, 143-144.
18. Havig, P., McIntire, J., and Geiselman, E., "Virtual Reality in a Cave: Limitations and the Need for HMDs?," *SPIE Defense, Security, and Sensing*, International Society for Optics and Photonics, May 2011, 804107.
19. Juan, M. and Pérez, D., "Comparison of the Levels of Presence and Anxiety in an Acrophobic Environment Viewed via HMD or CAVE," *Presence* 18(3):232-248, 2009.
20. Slater, M., Usoh, M., and Steed, A., "Depth of Presence in Virtual Environments," *Presence* 3(2):130-144, 1994.
21. Aykent, B., Yang, Z., Merienne, F., and Kemeny, A., "Simulation Sickness Comparison between a Limited Field of View Virtual Reality Head Mounted Display (Oculus) and a Medium Range Field of View Static Ecological Driving Simulator (Eco2)," *Driving Simulation Conference Europe 2014 Proceedings*, Society for Modeling & Simulation International, 2014, 65-71.
22. D-BOX, [http://www.d-box.com/fr/industrial/technology\\_products/index.html?actuators/index.ht](http://www.d-box.com/fr/industrial/technology_products/index.html?actuators/index.ht), 2015.
23. Aykent, B., Merienne, F., Paillot, D., and Kemeny, A., "Influence of Inertial Stimulus on Visuo-Vestibular Cues Conflict for Lateral Dynamics at Driving Simulators," *J Ergonomics* 3(113):2, 2013.
24. Meywerk, M., Aykent, B., and Tomaske, W., "ELBA: Das elektronische BASt-Archiv," 2009.
25. XSens Technologies BV15, "MTI and MTX User Manual and Technical Documentation," Document mt0100p, Revision o, 2010.
26. MathWorks, "MATLAB: Curve Fitting Toolbox; User's Guide," MathWorks, 2014.
27. MathWorks, "MATLAB: Statistics Toolbox; User's Guide," MathWorks, 2014.